

# Positron emission tomography (PET) and single photon emission computed tomography (SPELT) imaging of macrophages in large vessel vasculitis

Jiemay, William Febry; Heeringa, Peter; Kamps, Jan A. A. M.; van der Laken, Conny J.; Slart, Riemer H. J. A.; Brouwer, Elisabeth

*Published in:*
Autoimmunity reviews

*DOI:*
10.1016/j.autrev.2018.02.006



*Document Version*
Publisher's PDF, also known as Version of record

*Publication date:*
2018

Autoimmunity Reviews 17 (2018) 715–726

Contents lists available at ScienceDirect

Autoimmunity Reviews

journal homepage: www.elsevier.com/locate/autrev

Review

# Positron emission tomography (PET) and single photon emission computed tomography (SPECT) imaging of macrophages in large vessel vasculitis: Current status and future prospects

William Febry Jiemy [a,b], Peter Heeringa [a], Jan A.A.M. Kamps [a], Conny J. van der Laken [c], Riemer H.J.A. Slart [d,e], Elisabeth Brouwer [f,*]

[a] Department of Pathology and Medical Biology, University of Groningen, University Medical Center Groningen, Groningen, The Netherlands
[b] Faculty of Applied Science, UCSI University, UCSI Heights, Cheras, Kuala Lumpur, Malaysia
[c] Department of Rheumatology, Amsterdam Rheumatology and Immunology Center, VU University Medical Center, Amsterdam, The Netherlands
[d] Medical Imaging Center, Department of Nuclear Medicine and Molecular Imaging, University Medical Center Groningen, University of Groningen, Groningen, The Netherlands
[e] Department of Biomedical Photonic Imaging Group, University of Twente, Enschede, The Netherlands
[f] Department of Rheumatology and Clinical Immunology, University of Groningen, University Medical Center Groningen, Groningen, The Netherlands

ARTICLE INFO

*Article history:*
Received 2 February 2018
Accepted 7 February 2018
Available online 3 May 2018

*Keywords:*
Giant cell arteritis
Large vessel vasculitis
Positron emission tomography
Macrophage
Inflammation
Single photon emission computed tomography

ABSTRACT

Macrophages are key players in the pathogenesis of large-vessel vasculitis (LVV) and may serve as a target for diagnostic imaging of LVV. The radiotracer, $^{18}$F-FDG has proven to be useful in the diagnosis of giant cell arteritis (GCA), a form of LVV. Although uptake of $^{18}$F-FDG is high in activated macrophages, it is not a specific radiotracer as its uptake is high in any proliferating cell and other activated immune cells resulting in high non-specific background radioactivity especially in aging and atherosclerotic vessels which dramatically lowers the diagnostic accuracy. Evidence also exists that the sensitivity of $^{18}$F-FDG PET drops in patients upon glucocorticoid treatment. Therefore, there is a clinical need for more specific radiotracers in imaging GCA to improve diagnostic accuracy. Numerous clinically established and newly developed macrophage targeted radiotracers for oncological and inflammatory diseases can potentially be utilized for LVV imaging. These tracers are more target specific and therefore may provide lower background radioactivity, higher diagnostic accuracy and the ability to assess treatment effectiveness. However, current knowledge regarding macrophage subsets in LVV lesions is limited. Further understanding regarding macrophage subsets in vasculitis lesion is needed for better selection of tracers and new targets for tracer development. This review summarizes the development of macrophage targeted tracers in the last decade and the potential application of macrophage targeted tracers currently used in other inflammatory diseases in imaging LVV.



**Contents**

1. Introduction . . . 716
2. Large-vessel vasculitis (LVV) . . . 716
   2.1. Pathogenic model of large-vessel vasculitis . . . 716
      2.1.1. Vascular dendritic cell (vasDC) activation . . . 716
      2.1.2. Recruitment, activation and polarisation of CD4$^+$ T-cells . . . 716
      2.1.3. Recruitment and activation of monocyte . . . 717
      2.1.4. Vascular remodeling . . . 717
   2.2. Macrophages in vasculitis . . . 717
   2.3. The importance of macrophage targeted imaging in the diagnosis of LVV . . . 717
3. Positron emission tomography (PET) and single photon emission computed tomography (SPECT) . . . 718
4. Macrophage targeted PET and SPECT radio-tracers . . . 718

* Corresponding author at: University Medical Center Groningen, Department of Rheumatology and Clinical Immunology, AA21, Hanzeplein 1, P.O. Box 30001, 9700 RB Groningen, The Netherlands.
*E-mail address:* e.brouwer@umcg.nl (E. Brouwer).

https://doi.org/10.1016/j.autrev.2018.02.006

4.1. Clinically investigated macrophage targeted tracers for large vessel vasculitis . . . 718
4.1.1. Glucose metabolism targeted $^{18}$F-FDG PET . . . 718
4.1.2. Translocator protein (TSPO) targeted imaging . . . 719
4.2. Macrophage targeted tracers investigated in other inflammatory diseases . . . 720
4.2.1. Macrophage targeted radiotracers in clinical studies . . . 721
4.2.2. Macrophage targeted radiotracers in preclinical studies . . . 722
5. Future directions and theranostic applications . . . 722
6. Concluding remarks . . . 723
Take-home messages . . . 723
Conflict of interest . . . 723
References . . . 723

## 1. Introduction

The human blood vessel system is one of the largest organ systems in the human body [1,2]. As part of the cardiovascular system, the blood vessel system functions by distributing blood cells, oxygen and nutrients to, as well as expelling waste such as carbon dioxide from, all organs and tissues. Separately, in the lymphoid system, blood vessels act as the transit site of lymphoid and myeloid cells of the immune system. Given the importance of blood vessels, inflammation of the vessels (vasculitis) can have major health consequences. The Chapel Hill Consensus Conference in 2012 revised the nomenclature of the primary vasculitides and classified vasculitis based on the size of the vessels involved into small-vessel vasculitis (SVV), medium-vessel vasculitis (MVV), large-vessel vasculitis (LVV) and variable-vessel vasculitis (VVV) [3]. LVV is a disease marked by inflammation of the vessel wall that progresses to vascular remodeling and thickening of the vessel wall causing stenosis, occlusion or dilatation of the vessels which may result in ischemic complications such as sight loss, stroke and aneurysms. Therefore, early recognition of LVV is crucial.

Nuclear imaging is currently gaining importance as a non-invasive tool for the diagnosis and monitoring of vascular inflammation. The application of nuclear imaging in the detection of LVV was initially a serendipitous discovery by Blockmans et al. [4]. In their study, the authors compared $^{18}$F-Fluorodeoxyglucose positron emission tomography ($^{18}$F-FDG PET) and Gallium-68 scintigraphy in patients with fever of unknown origin (FUO) and found vascular uptake in patients with underlying vasculitis. Given the limited resolution of nuclear imaging cameras, these techniques are more efficient in the assessment of LVV but not MVV or SVV [5]. However, recent studies have also indicated the potential role of new PET camera systems (up to 2 mm resolution) in the detection of organ involvement in MVV and SVV [6–9].

Macrophages have been recognized as key cellular players in the pathogenesis of LVV. Circulating monocytes are recruited to vasculitic lesions where they are activated and differentiate into macrophages. These activated macrophages produce pro-inflammatory cytokines and chemokines which amplify the inflammatory response and induce vascular remodeling [2,10]. $^{18}$F-FDG PET as a tool for imaging inflammation has already proven to be useful for early diagnosis of LVV (within 3 days of glucocorticoid treatment – sensitivity and specificity may drop afterwards). However, $^{18}$F-FDG is less useful for monitoring disease progression and evaluating therapy responses due to a dramatic drop in diagnostic accuracy in patients undergoing glucocorticoid treatment and inability to differentiate long lasting vessel wall remodelling with active vasculitis. Better and more specific macrophage targeted radiotracers are therefore needed to improve diagnostic accuracy and treatment monitoring especially in patients with ongoing glucocorticoid treatment. Following a brief overview of LVV pathogenesis, this review summarises the development of macrophage targeted tracers in the last decade using two different nuclear imaging approaches – positron emission tomography (PET) and single photon emission computed tomography (SPECT) imaging. Moreover, the potential application of tracers currently used in other inflammatory diseases in imaging macrophages in LVV is discussed as well.

## 2. Large-vessel vasculitis (LVV)

LVV includes two pathological conditions: giant cell arteritis (GCA) and Takayasu arteritis (TAK). The pathogenesis of both GCA and TAK involves inflammation, often granulomatous, of large to medium size arteries (aorta and its major branches). GCA generally occurs in older Caucasian female individuals (≥50 years old) of Scandinavian descent in Europe and Minnesota. The disease usually affects the aorta and its major branches with a predilection towards carotid and vertebral arteries although other types of arteries can also be affected. GCA belongs to a clinical disease spectrum which includes cranial GCA (C-GCA) and large-vessel GCA (LV-GCA) [3,11,12]. LV-GCA often overlaps with polymyalgia rheumatica (PMR), another inflammatory disorder of the elderly, affecting muscles marked by pain and stiffness in the neck, shoulder and hip region. Studies have shown that 40–60% GCA patients may have PMR and according to the literature, up to 21% of PMR patients may develop GCA [11,17]. TAK, on the other hand, is more common in younger Asian females (≤50 years old) [3,13,14]. GCA and TAK have a similar clinical presentation including fever of unknown origin (FUO), headache, malaise, anorexia, weight loss and in the progressive phase of the disease, symptoms of occlusion and aneurysm. Histopathological features in the affected vessels of GCA and TAK are overlapping and thus the only factor distinguishing GCA and TAK is geographical distribution and the age of onset [11,14–17].

### 2.1. Pathogenic model of large-vessel vasculitis

The etiology of LVV is unknown. However, based on clinical and experimental investigations, a pathogenic model for disease development and progression has been proposed which includes four phases.

#### 2.1.1. Vascular dendritic cell (vasDC) activation

Vascular dendritic cells (vasDC) are sentinel immune surveillance cells located in the adventitia of the artery. When no inflammation occurs, resting vasDc are CD83$^-$MHC-II$^{low}$. In the event of vasculitis, vasDC are activated through the stimulation of toll-like receptors (TLRs) by a factor yet to be identified. Studies have shown increased expression of TLR 2 and TLR 4 on vasDC of vasculitis patients. Activation of vasDC by TLR 4 ligands changes the phenotype of vasDc into CD83$^+$MHC-II$^{high}$ and induces the production of chemokines such as CCL18, CCL19, CCL20, CCL21 and cytokines such as IL-1β, IL-6, IL-18, IL-23 and IL-33. These chemokines and cytokines are responsible for the recruitment and polarisation of CD4$^+$ T-cells in addition to promoting angiogenesis [2,18–20].

#### 2.1.2. Recruitment, activation and polarisation of CD4$^+$ T-cells

The chemokines produced by activated vasDC (CCL18, CCL19, CCL20, CCL21) recruit CD4$^+$ T-cells, which enter the adventitia through the *vasa vasorum*. Recruited CD4$^+$ T-cells are then activated through

docking of T-cell receptors (TCRs) to MHC-II on vasDC – presenting a still unknown antigen. Upon activation, T-cells differentiate into different subtypes depending on the presence of specific cytokines in the micro-environment. The cytokines IL-12 and IL-l8 polarise the T-cells into T helper 1 (Th1) subtype. Th1 cells produce interferon-γ (IFN-γ), a very powerful pro-inflammatory cytokine that is important for macrophage activation, production of pro-inflammatory cytokines and chemokines, and production of vascular endothelial growth factor (VEGF). VEGF then activates vascular smooth muscle cells (VSMCs) and endothelial cells (ECs) promoting vascular remodeling, neoangiogenesis, production of chemokines (CCL2, CX3CL1 CXCL9, CXCL10 and CXCL11) for recruitment of monocytes and T-cells, and T-cell activation via the NOTCH-NOTCH ligand activation pathway [2,18–21]. On the other hand, cytokines like IL-1β, IL-6, IL-21 and IL-23 polarise T-cells into T helper 17 (Th17) subtype, which produce pro-inflammatory cytokines and chemokines such as IL-17, IL-21, IL-22, IL-26 and CCL20. IL-17 is a potent pro-inflammatory cytokine that exerts its effect by activating VSMCs and ECs inducing production of chemokines (CCL2, CCL20, CXCL1, CXCL2, CXCL5 and CXCL8) that subsequently promote the recruitment of T-cells, monocytes and neutrophils. IL-17 also induces the production of cytokines such as IL-1β, IL-6, IL-21 and IL-23 by macrophages and vasDCs, thus stabilizing the Th17 lineage. IL-21 induces activation of natural killer cells (NK cells), the differentiation of cytotoxic $CD8^+$ T-cells and the differentiation of Th17 cells. IL-22 is responsible for induction of an acute phase reaction while the chemokine CCL20 facilitates the recruitment of $CD4^+$ T-cells and dendritic cells. The IL-6-IL-17 Th17 pathway is sensitive to glucocorticoid (GC) treatment. However, in the chronic phase of LVV, the IFN-γ Th1 pathway is dominant and is unaffected by GC treatment [2,18–20].

#### 2.1.3. Recruitment and activation of monocyte

Monocytes are divided into three subtypes namely the classical monocytes (marked by $CD14^{bright}CD16^-$), intermediate monocytes (marked by $CD14^{bright}CD16^+$) and non-classical monocytes (marked by $CD14^{dim}CD16^+$). Classical monocytes express CCR2, which is the receptor for CCL2 while the $CD16^+$ intermediate and non-classical subsets express CX3CR1, a receptor for CX3CL1 [23]. Activation of ECs and VSMCs by IFN-γ and IL-17 lead to the production of CCL2 and CX3CL1, which in turn promote the recruitment of circulating monocytes to the vasculitic lesions [19,23]. Due to the presence of various cytokines in the microenvironment, recruited monocytes become activated and differentiate into macrophages. These macrophages, some of which merge into multi-nucleated giant cells, produce a wide range of pro-inflammatory cytokines and growth factors that activate the VSMCs, ECs and T-cells and thus amplify the inflammatory response. Growth factors produced by activated macrophages are also responsible for vascular remodeling and angiogenesis. Moreover, activated macrophages also produce reactive oxygen species and matrix metalloproteinases (MMPs), which are responsible for tissue destruction [18,19,22,24,25].

#### 2.1.4. Vascular remodeling

Macrophages activated by IFN-γ produce VEGF and platelet derived growth factors (PDGF). PDGF activates VSMCs by promoting their migration towards the intima of the vessels and inducing their proliferation leading to intimal hyperplasia, occlusion and ischemic complications. Activated macrophages and VSMCs also produce MMPs namely MMP-9 and MMP-2, which digest elastin in the internal elastic lamina leading to destruction of the media. VEGF and IL-33 produced by activated DCs and macrophages are the main effectors of neoangiogenesis. In LVV, the *vasa vasorum* is reported to infiltrate the media and intima promoting the migration and recruitment of inflammatory cells. Taken together, these processes initiate an inflammatory amplification loop that enhances tissue destruction and vascular remodeling which ultimately results in ischemic complications [18,19,24].

### 2.2. Macrophages in vasculitis

Macrophages are generally divided into two major subtypes: classically activated macrophages (M1) and alternatively activated macrophages (M2). Depending on the cytokines in the microenvironment, macrophages are polarised into these distinct subtypes. M1 macrophages are considered pro-inflammatory that are generated through Th1 responses. This subtype is activated by IFN-γ and produces pro-inflammatory cytokines such as IL-1β, IL-6, IL-12 and IL-23; growth factors such as VEGF and PDGF; MMPs; and reactive oxygen species whose functions are clearly important in the pathogenesis of LVV [24,26,27].

M2 macrophages, known as the anti-inflammatory and tissue repairing subtype, are divided into four subsets: M2a, M2b, M2c and M2d macrophages. IL-4 and IL-13 polarise macrophages into M2a subsets, immune complexes, TLR and IL-1R ligands polarise macrophages into M2b subsets while IL-10, TGF-β and glucocorticoids polarise macrophages to M2c subsets. These three subsets are marked by production of IL-10 and upregulation of the macrophage mannose receptor (MMRs/CD206) [24,26–28]. The M2d subset is induced by IL-6 and produces high levels of VEGF, IL-10, IL-12, TNF-α and TGF-β. This subset might be important in the pathogenesis of LVV corresponding to high levels of IL-6 in GCA patients. Recently, another subset activated by IL-17 was identified. Similar to M1 macrophages, this subset produces pro-inflammatory cytokines but also showed upregulation of the scavenger receptor CD163, a marker for M2 polarisation [28,29]. Important to note is that the classification of macrophages into M1/M2 subsets is based on *in vitro* models under specific and controlled conditions that may not mirror macrophage behavior *in vivo*. It is well known that macrophages are remarkably plastic and can easily change phenotypes depending on the signals they receive in their microenvironment [24,28,30]. Reports also indicate that macrophages in pathological conditions may show an intermediate phenotype with mixed M1 and M2 characteristics [31].

Arguably, M1 macrophages would be expected to be the dominant subset in vasculitic lesions given their role in the inflammatory amplification loop in LVV. However, Ciccia et al. reported that both M1 and M2 macrophages are significantly expanded in the inflamed arteries of GCA patients [32]. The roles of M2 subsets in vasculitis have yet to be investigated but it has been suggested that M2 macrophages may contribute to giant cell formation, angiogenesis and vascular remodeling [24]. Currently, there is a lack of knowledge regarding the detailed phenotypes and subset distribution of macrophages in vasculitic lesions in LVV. A more detailed knowledge of macrophage subsets/phenotypes in early and chronic vasculitic lesions may shed light on their specific role in LVV pathogenesis.

### 2.3. The importance of macrophage targeted imaging in the diagnosis of LVV

Currently, diagnosis of GCA and TAK relies heavily on the assessment of clinical symptoms, laboratory assessment of acute phase reaction protein levels [C-reactive protein (CRP), erythrocyte sedimentation rate (ESR)] and levels of serum IL-6 [11,15–17]. In 1990, the American College of Rheumatology (ACR) developed criteria for the classification of GCA and TAK to discriminate GCA and TAK from other types of vasculitis [12,13]. While these criteria were not intended for the diagnosis of the diseases, they have been widely misused as a diagnostic tool. To date, the golden standard for GCA diagnosis is a positive temporal artery biopsy (TAB). However, inflammatory lesions in GCA arteries often are patchy and focal in nature which may lead to a false negative result if the biopsy was taken from a non-inflamed region. TAB is also not useful in LV-GCA without temporal artery involvement. The use of color Doppler ultrasonography (CDUS) in the diagnosis of GCA has also been applied. CDUS of inflamed artery produces a “halo” sign at regions with thickening of the vessel wall. Magnetic resonance angiography (MRA) and computed tomography angiography (CTA) are likewise useful in the assessment of artery involvement, disease extent and assessment

of vascular damage particularly in patients with an established diagnosis of GCA [33,34,37]. In the case of TAK, diagnosis is usually carried out via arteriographies such as CDUS, CTA and MRA [35,36].

Given that macrophages dominate the cellular infiltrate in vasculitic lesions, imaging macrophages *in vivo* may prove to be very useful in the diagnosis and tracking of disease activity and progression in LVV. Biopsies may yield a false negative diagnosis as a result of the focal nature of GCA lesions. Ultrasonography and angiography by means of CDUS, MRA or CTA can only detect GCA lesions after morphological changes (later phase). PET on the other hand, has proven to be more useful in detecting early inflammatory stages of vasculitis [37–39]. $^{18}$F-FDG PET signal intensity has been found to be strongly associated with macrophage density [40–42]. Activated macrophages and lymphocytes overexpress glucose transporters (Glut-1 and Glut-5) and undergo a switch to glycolysis. Based on this principle, $^{18}$F-FDG, a radiolabelled glucose analog, is highly taken up by infiltrating immune cells (including macrophages) in active vasculitic lesions. In the past decade, $^{18}$F-FDG PET has proven to be an efficient method for the diagnosis of GCA, TAK and large-vessel involvement in PMR patients. However, $^{18}$F-FDG is not specific as it is also taken up by other proliferating cells. Reports have also indicated higher $^{18}$F-FDG uptake in aging vessels due to changes of metabolic activity, persistent vessel wall remodeling and atherosclerotic calcifications which may further affect diagnostic accuracy [43,44]. Therefore, more specific radiotracers are needed. With extensive research currently being done on developing new radiotracers specifically targeting macrophages, nuclear imaging may not only provide a non-invasive tool for the diagnosis of LVV but may also be useful in assessing disease progression and effectiveness of treatment in reducing vessel wall inflammation.

## 3. Positron emission tomography (PET) and single photon emission computed tomography (SPECT)

PET and SPECT are nuclear imaging techniques based on detection of gamma rays [45,46]. Of all existing *in vivo* imaging techniques, PET and SPECT have the highest sensitivity – up to picomolar level for PET and nanomolar level for SPECT – while other techniques such as MRI can only achieve milli to micromolar sensitivity. Despite their superior sensitivity, spatial resolution of PET and SPECT is limited and anatomical information is poor when compared to other techniques making PET/SPECT less useful for imaging medium to small vessels (<4 mm) [45,47,48]. However, the ability of PET and SPECT to visualize functional information *in vivo* is important for early diagnosis and disease assessment. Since MR or CT can provide morphological information and better spatial resolution, these modalities are often combined in a single PET/CT, PET/MR or SPECT/CT camera system, referred to as hybrid imaging. These combinations provide an improvement to the limited spatial resolution of PET and SPECT [46,49]. Using combined PET/CT, Gaemperli et al. successfully detected temporal artery inflammation in GCA patients [50]. The combination of these modalities is also important to obtain accurate molecular and anatomical image co-registration, including soft tissue attenuation correction, for accurate quantification of radiotracers in target tissues [49].

Besides the similarities between PET and SPECT, each modality also offers specific advantages. The main advantage of PET over SPECT is its higher sensitivity, spatial resolution and the ability of absolute quantification. Another advantage of PET is that the radiotracers are identical to the non-radioactive counterparts (*i.e.* substitution of $C^{12}$ with $C^{11}$) [45,51]. With regard to background noise, Takahashi et al. compared PET and SPECT by using $^{90}$Y, a radionuclide that can be used for both PET and SPECT, and showed that PET produced superior images compared to SPECT due to lower background noise [52]. However, SPECT also offers some advantages over PET. SPECT radionuclides generally have longer half-lives compared to PET radionuclides making them more suitable for labelling larger biomolecules such as peptides and antibodies. As larger biomolecules have a slower rate of tissue penetration – translating to a longer time for the radiotracers to reach target tissues – the longer half-lives of SPECT radiotracers allow the measurement of slow kinetic processes that might take hours or days to achieve [45,53] Nevertheless, emerging PET radionuclides such as $^{64}$Cu and $^{89}$Zr have longer half-lives, comparable to SPECT radionuclides, and are gaining popularity for antibody tagging (immuno-PET). Despite the multiple advantages of PET over SPECT, PET should not be assumed to be the preferred method of nuclear imaging. This is because SPECT scanners are more widely available, SPECT scans are relatively inexpensive and production of SPECT radiotracers is independent of a cyclotron. Additionally, recent advances in gamma cameras have improved the resolution and sensitivity of SPECT although spatial resolution of PET is still comparatively higher [46,54]. In daily practice, the design of radiotracers to be used for nuclear imaging between these two modalities is mainly based on the availability of the machines, cost and the target molecule to be tagged.

## 4. Macrophage targeted PET and SPECT radio-tracers

Since macrophages are key players of various inflammatory disorders and oncological conditions, they are considered an important target for nuclear imaging both for diagnosis and assessment of treatment effectiveness. The importance of macrophage targeting is also emphasized by the recent increase in research and development of new radiotracers targeting various biological pathways and markers on macrophages for LVV and other related inflammatory diseases (Fig. 1).

### *4.1. Clinically investigated macrophage targeted tracers for large vessel vasculitis*

To date, the only radiotracer used in clinics for diagnosis of LVV is $^{18}$F-FDG. Macrophage targeted radiotracers targeting translocator protein (TSPO) have also been tested in LVV imaging showing promising results emphasizing the suitability of macrophage targeted radiotracers for imaging LVV.

#### *4.1.1. Glucose metabolism targeted $^{18}$F-FDG PET*

Since the discovery of the usefulness of $^{18}$F-FDG PET in diagnosis of LVV by Blockmans et al., this radiotracer has been widely employed for diagnosing GCA and TAK. However, consensus guidelines for the interpretation of scan results are currently lacking. Table 1 summarises the methods currently used for interpretation of $^{18}$F-FDG PET scan results in LVV. In a recent study by Stellingwerf et al., different scoring methods for $^{18}$F-FDG PET scans in GCA patients were compared [59]. The group concluded that the visual grading system with grade 3 uptake (higher than liver uptake) yielded the highest diagnostic accuracy for qualitative method (sensitivity of 83% and specificity of 91%) while standardized uptake value (SUVmax) aorta to liver ratio was the superior semi-quantitative method (cut-off value of 1.03, sensitivity of 72% and specificity of 92%). However, diagnostic accuracy dropped dramatically in patients undergoing glucocorticoid treatment. A recent study by Clifford et al. indicated a sensitivity and specificity of only 71.4% and 64.3% respectively in GCA patients after only 12 days of glucocorticoid treatment [60]. Thus, although $^{18}$F-FDG PET has been proven a useful tool for diagnosis of LVV, more specific radiotracers are needed to improve diagnostic accuracy especially in patients undergoing glucocorticoid treatment. Additionally, in regards to disease monitoring, Blockmans et al. also published their findings on repetitive $^{18}$F-FDG PET scan on GCA patients undergoing glucocorticoid treatment where lower $^{18}$F-FDG uptake was shown compared to baseline and 3 months after treatment but no further reduction was shown after 6 months of treatment in patients with and without a disease flare [61]. However, these results appear inconsistent with recent observations by Malezewski et al. in repeat temporal artery biopsies demonstrating a time-dependent decrease of macrophage rich granulomatous

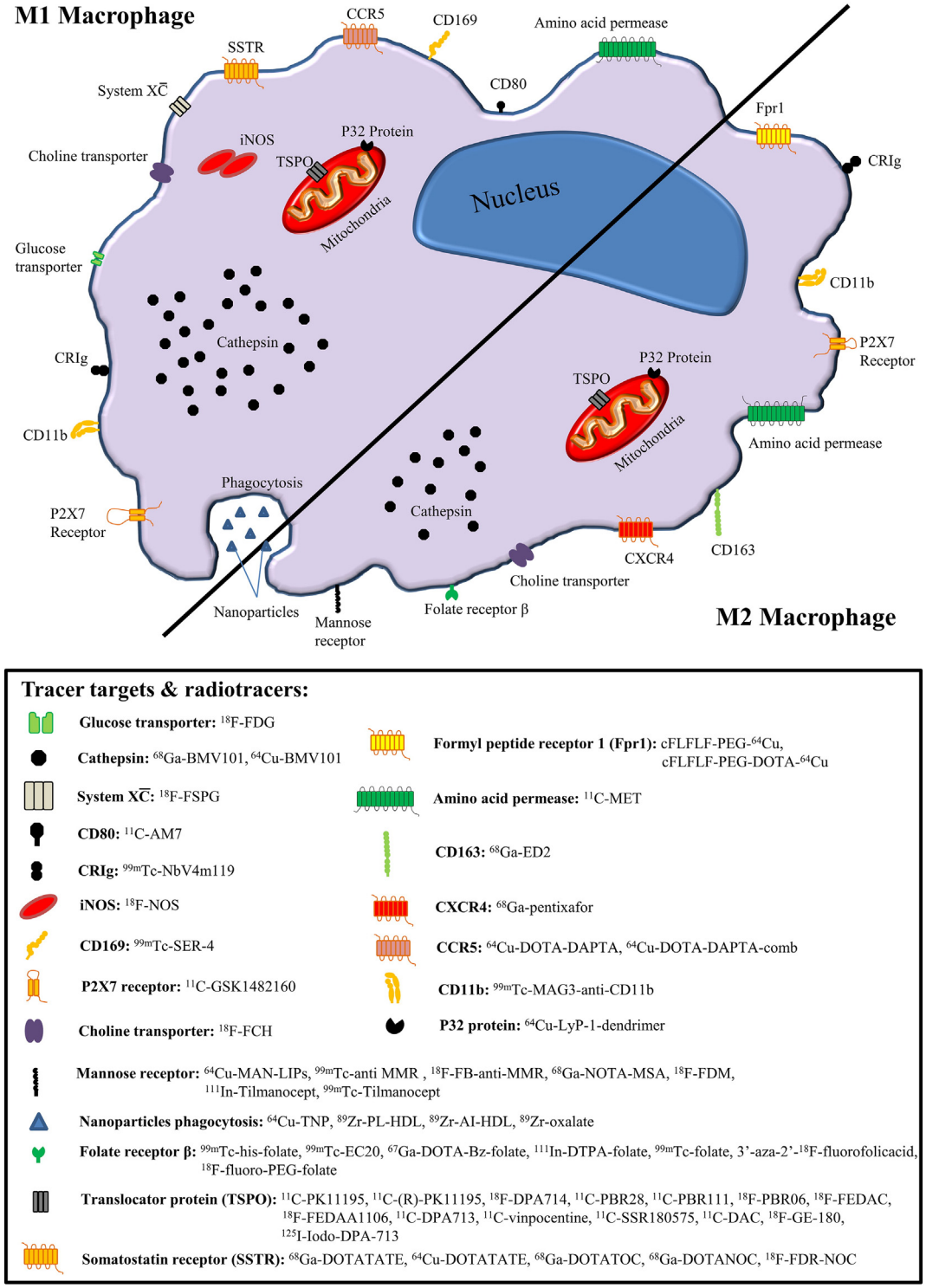


**Fig. 1.** Distribution of macrophage specific radiotracers targets. These biomarkers are generally expressed in all activated macrophages. However, some markers are highly upregulated on M1 macrophage while the others are expressed more on M2 macrophages. This figure showed the expression of the markers based on dominant expression on M1 and M2 subset.

inflammation in GCA patients upon glucocorticoid treatment of 50% and 25% after 9 and 12 months respectively [62]. This inconsistency might be caused by $^{18}$F-FDG uptake by other persistent infiltrating lymphocytes in the vessels despite reduction in inflammation. In addition, higher $^{18}$F-FDG uptake has also been reported in aging vessels due to changes in metabolic activity, vessel wall remodeling and atherosclerosis [43,44]. Therefore, more specific macrophage targeted radiotracers are also needed for better visualisation of reduced inflammation and treatment monitoring.

*4.1.2. Translocator protein (TSPO) targeted imaging*

For over 20 years, macrophage targeted radiotracers targeting translocator protein (TSPO; also known as PBR or peripheral benzodiazepine receptor) have been used in PET imaging for neuroinflammatory diseases (Table 3). TSPO is a 18 kDa protein expressed on the outer membrane of mitochondria. Although TSPO is expressed in both M1 and M2 subsets, some reports have shown higher expression in M2 macrophages [63,64]. In more recent studies, targeting TSPO receptors

**Table 1**
Summary of $^{18}$F-FDG PET scoring methods in LVV diagnosis.

| Method | Description | Reference |
|---|---|---|
| Qualitative | First impression visual method based on expert opinion | [55] |
| Qualitative | Visual grading system based on four point scale (grade 0 = no vascular uptake, grade 1 = lower than liver uptake, grade 2 = similar to liver uptake, grade 3 = higher than liver uptake). | [56] |
| Semi quantitative | Ratio between the aortic wall standardized uptake value (SUVmax aorta) and liver uptake (SUVmax liver). | [57] |
| Semi quantitative | Ratio between the aortic wall standardized uptake value (SUVmax aorta) and lung uptake (SUVmax lung) or venous blood pool background (SUVmean venous blood pool). | [58] |

has shown promising results in imaging non-neuronal inflammatory diseases such as rheumatoid arthritis, atherosclerosis, GCA, TAK and systemic lupus erythematosus [65–67,69,72,77]. Pugliese et al. first tested $^{11}$C-PK11195, a TSPO targeted radiotracer, for LVV imaging in a small study involving fifteen patients with a systemic inflammatory disorder with a high suspicion of LVV [67]. Visual analysis showed focal vascular uptake in all six symptomatic patients as compared to no uptake in asymptomatic patients. Semi-quantitative analysis comparing the SUVmax aorta to the SUVmax venous blood pool revealed that all six symptomatic patients had individual target to background ratios (TBR) of >1.20 ($2.41 \pm 1.59$, $p = 0.001$) while all asymptomatic patients had TBR of <1.20. A PET/CT scan was repeated for one symptomatic patient after 20 weeks of glucocorticoid treatment and the result indicated a reduction of vascular $^{11}$C-PK11195 uptake in parallel with a reduction of serum inflammatory markers and clinical improvement. Furthermore, Lamare et al. tested $^{11}$C-(R)-PK11195 in individuals with systemic inflammation suspected of LVV (symptomatic, $n = 3$; asymptomatic, $n = 4$) [72] demonstrating a two-fold increase of vascular $^{11}$C-(R)-PK11195 uptake in symptomatic patients as compared to asymptomatic patients. These studies suggest the potential of targeting TSPO for LVV imaging and support the contention that targeting (M2) macrophages is feasible for imaging LVV. However, there is a disadvantage in targeting TSPO. Owen et al. found that in some patients, TSPO tracers were less efficient in binding to the target receptor [97,98]. Older generation TSPO targeted radiotracers such as PK11195 based tracers also have high background blood-pool accumulation which affects their accuracy. Nevertheless, new TSPO targeted radiotracers with improved binding characteristics compared to classic TSPO radiotracers have been developed and are currently being evaluated in pre-clinical studies although these new tracers exert various binding capability depending on TSPO polymorphism (Table 2).

### *4.2. Macrophage targeted tracers investigated in other inflammatory diseases*

To date, a number of macrophage targeted tracers are already available clinically or are being evaluated in clinical studies for oncological and other inflammatory diseases. In addition, many newly developed macrophage targeted tracers are currently emerging and are undergoing preclinical testing. Although these tracers have yet to be tested for

**Table 2**
List of TSPO targeted radiotracers in inflammatory disorders.

| Radiotracer | Modality | Clinical/preclinical | Disease | Reference |
|---|---|---|---|---|
| $^{11}$C-PK11195 | PET | Clinical | Multiple sclerosis | [65] |
| | PET | Preclinical | Neuro-inflammation | [66] |
| | PET/CT | Clinical | Systemic inflammation (predominantly GCA) | [67] |
| | PET | Preclinical | Neuro-inflammation | [68] |
| | PET/CT | Clinical | Atherosclerosis | [69] |
| | PET | Preclinical | Cerebral ischemia | [70] |
| $^{11}$C-(R)-PK11195 | PET | Clinical | Rheumatoid arthritis | [71] |
| | PET/CT | Clinical | Systemic inflammation (predominantly GCA) | [72] |
| | PET | Preclinical | Traumatic brain injury | [73] |
| | PET | Clinical | Multiple sclerosis | [74] |
| | PET | Preclinical | Lung inflammation | [75] |
| | PET | Preclinical | Liver damage | [76] |
| | PET | Clinical | Rheumatoid arthritis | [77] |
| | PET | Preclinical | Cerebral ischemia | [78] |
| $^{18}$F-DPA714 | PET | Preclinical | Neuro-inflammation | [66] |
| | PET | Preclinical | Abdominal aortic aneurysm | [79] |
| | PET | Preclinical | Multiple sclerosis | [80] |
| | PET | Preclinical | Cerebral ischemia | [70] |
| | PET | Preclinical | Peripheral tissue inflammation | [81] |
| | PET/CT | Preclinical | Rheumatoid arthritis | [82] |
| | PET/CT | Preclinical | Allograft rejection | [83] |
| | PET | Preclinical | Traumatic brain injury | [84] |
| $^{11}$C-PBR28 | PET | Clinical | Multiple sclerosis | [85] |
| | PET | Preclinical | Acute inflammation and adjuvant arthritis | [86] |
| $^{11}$C-PBR111 | PET | Preclinical | Epilepsy | [87] |
| | PET | Preclinical | Multiple sclerosis | [88] |
| | PET | Clinical | Multiple sclerosis | [89] |
| $^{18}$F-PBR06 | PET | Clinical | Quantification of brain TSPO expression | [90] |
| $^{18}$F-FEDAC | PET | Preclinical | Lung inflammation | [75] |
| | PET | Preclinical | Liver damage | [76] |
| $^{18}$F-FEDAA1106 | PET | Clinical | Multiple sclerosis | [91] |
| | PET | Preclinical | Atherosclerosis | [92] |
| $^{11}$C-DPA713 | PET | Preclinical | Neuro-inflammation | [66] |
| $^{11}$C-vinpocentine | PET | Clinical | Multiple sclerosis | [65] |
| $^{11}$C-SSR180575 | PET | Preclinical | Neuro-inflammation | [68] |
| $^{11}$C-DAC | PET | Preclinical | Multiple sclerosis | [93] |
| $^{18}$F-GE-180 | PET | Preclinical | Cerebral ischemia | [78] |
| $^{125}$I-Iodo-DPA-713 | SPECT/CT | Preclinical | Tuberculosis associated inflammation | [94] |
| | SPECT/CT | Preclinical | Atherosclerosis | [95] |
| | SPECT/CT | Preclinical | Chronic pancreatitis | [96] |

vasculitis, such radiotracers have potential to be used for macrophage imaging in LVV as well.

*4.2.1. Macrophage targeted radiotracers in clinical studies*

Besides targeting glucose metabolism and TSPO, macrophage targeted radiotracers targeting other biological pathways and receptors are already available for diagnosis and assessment of many other diseases (Table 3). These tracer targets are generally expressed in all activated macrophages. However, some target receptors or metabolic activities are higher in certain subsets of macrophages depending on the polarisation stimulus in the microenvironment. Therefore, some of these tracers are more suitable to target M1 macrophage while others preferentially target M2 macrophages. As mentioned earlier, macrophages are incredibly plastic and switch phenotypes governed by factors in the microenvironment. Therefore, although these radiotracers have potential to be utilized for LVV imaging, their suitability needs to be further investigated as macrophages in LVV lesion might express different targets compared to other diseases.

Several macrophage surface receptors are gaining importance in imaging inflammatory diseases. One of the target surface receptors for macrophage targeted imaging is the somatostatin receptor (SSTR). SSTRs are G-protein coupled receptors expressed throughout various tissues and by cells of the immune system. Recently, Tarkin et al. assessed the expression of SSTR2 on macrophages subsets and found higher expression on M1 macrophages [103]. In recent studies by Gormsen et al. and Tarkin et al., $^{68}$Ga-DOTANOC and $^{68}$Ga-DOTATATE displayed superior specificity, sensitivity and accuracy in imaging cardiac sarcoidosis and atherosclerosis in patients compared to $^{18}$F-FDG due to lower background noise [102,103]. Another surface receptor, the macrophage mannose receptor (MMR/CD206), is considered a hallmark of M2 macrophages is also utilized as tracer target. In an attempt to understand HIV associated vascular inflammation, research by Zanni et al. revealed a higher uptake of the MMR specific SPECT tracer $^{99m}$Tc-Tilmanocept in the aorta of HIV patients compared to non-HIV controls and demonstrated co-localisation of $^{99m}$Tc-Tilmanocept with CD206$^{+}$ macrophages [104]. Recently, a CXCR4 specific PET radioligand, $^{68}$Ga-Pentixafor, has been developed for cancer imaging. CXCR4 is chemokine receptor belonging to the family of G-protein coupled receptors that are expressed on immune cells and is upregulated in various oncological conditions [105–107]. Hyafil et al. used this radioligand to successfully image atherosclerosis in atherosclerosis patients [107]. They found that there was focal uptake of $^{68}$Ga-Pentixafor in atherosclerotic lesions and no uptake in asymptomatic controls. Another receptor, namely the folate receptor, is also currently emerging as a potential target for imaging tumours and inflammatory diseases. Physiologically, folate is an important compound that is critical for DNA and RNA synthesis. There are three different Folate receptors subtypes namely FR-α, FR-β and FR-γ. While these folate receptors are expressed in various tissues, the active form of the FR-β is exclusively expressed on all activated macrophages, and association has been described with the M2 subtype [108–110]. Matteson et al. successfully imaged inflamed joints in rheumatoid arthritis patients with FolateScan™ ($^{99m}$Tc-EC20) albeit with low sensitivity (40%) [112].

Apart from surface receptors, some tracers target biological pathways. Similar to imaging glucose uptake in $^{18}$F-FDG PET, radiolabelled choline has been used to target macrophages and tumours. Choline is a precursor of phosphatidylcholine, a major constituent of the cell membrane with increased choline uptake by tumours and activated macrophages at inflammatory sites having been previously reported [111]. Vöö and colleagues imaged atherosclerotic patients with $^{18}$F-FCH (fluorocholine) revealing a higher uptake in symptomatic plaques compared to asymptomatic plaques that were highly correlated with macrophage infiltration [108].

Another pathway utilized in macrophage targeting involves system X$\bar{C}$. System X$\bar{C}$ is a cell membrane transporter that functions in cysteine/glutamate uptake and its expression is reported to be upregulated in LPS and IFN-γ induced M1 macrophages [113,114]. Chae et al. imaged a $^{18}$F labelled glutamate derivative, $^{18}$F-FSPG, that is specifically taken up by system X$\bar{C}$, in sarcoidosis patients [115]. Their findings showed a higher radiotracer uptake in sarcoidosis patients than in non-sarcoidosis patients. Additionally, compared to $^{18}$F-FDG, $^{18}$F-FSPG demonstrated significantly lower background uptake. Another radiotracer, $^{11}$C-Methionine ($^{11}$C-MET), a well-established radiotracer for neuro-oncological diseases is also rising in imaging inflammatory diseases. The principle behind $^{11}$C-MET PET is that proliferating cells have elevated amino acid uptake and studies have reported that infiltrating macrophages in tumour lesions showed increased methionine uptake [116]. The first report of $^{11}$C-MET in inflammatory disease was reported by Morooka et al. where the group imaged nine patients with myocardial infarction and found $^{11}$C-MET uptake in infarct regions [117]. Recent reports also showed a 7 fold increase of $^{11}$C-MET in M1 macrophages in comparison to M2 macrophages and lower background uptake compared to $^{18}$F-FDG [118,119].

Upon activation, certain enzymes are upregulated in macrophages which can therefore be utilized as tracer targets. Two of such enzymes are inducible nitric oxide synthase (iNOS) and cathepsin. The enzyme iNOS synthesizes Nitric oxide (NO) that is highly upregulated in M1 macrophages and has been widely used as a marker for M1 macrophages [120–122]. Huang et al. synthesized a novel iNOS specific radiotracer for PET imaging referred to as $^{18}$F-NOS and tested the tracer in a human model of lung inflammation (endotoxin instillation) [123]. It was found that there was a 30% increased radiotracer uptake after endotoxin-induced lung inflammation compared to baseline. On the other hand, cathepsins are cysteine proteases that are highly expressed in macrophages. While cathepsins are expressed in both M1 and M2 macrophages, studies have shown that expression levels are higher in

**Table 3**
Macrophage targeted radiotracers in clinical studies.

| Tracer target | Dominant macrophage subset | Radiotracer | Type | Modality | Disease | Reference |
|---|---|---|---|---|---|---|
| Somatostatin receptor (SSTR) | M1 | $^{68}$Ga-DOTATATE | Chemical | PET/CT | Atherosclerosis | [99] |
| | | $^{64}$Cu-DOTATATE | Chemical | PET/MR | Atherosclerosis | [100] |
| | | $^{68}$Ga-DOTATOC | Chemical | PET/MR | Atherosclerosis | [100] |
| | | $^{64}$Cu-DOTATATE | Chemical | PET/CT | Atherosclerosis | [101] |
| | | $^{68}$Ga-DOTANOC | Chemical | PET/CT | Cardiac sarcoidosis | [102] |
| | | $^{68}$Ga-DOTATATE | Chemical | PET/CT | Atherosclerosis | [103] |
| Macrophage mannose receptor (MMR/CD206) | M2 | $^{99m}$Tc-Tilmanocept | Chemical | SPECT/CT | Arterial inflammation | [104] |
| CXCR4 (CD184) | M2 | $^{68}$Ga-pentixafor | Chemical | PET/MR | Atherosclerosis | [107] |
| Choline metabolism | M1/M2 | $^{18}$F-FCH | Chemical | PET/CT | Atherosclerosis | [111] |
| Folate receptor beta (FR-β) | M2 | $^{99m}$Tc-EC20 | Chemical | SPECT | Rheumatoid arthritis | [112] |
| System X$\bar{C}$(cysteine/glutamate antiporter) | M1 | $^{18}$F-FSPG | Chemical | PET/CT | Sarcoidosis | [115] |
| Amino acid metabolism | M1 | $^{11}$C-methionine | Amino acid | PET | Myocardial infarction | [117] |
| Inducible nitric oxide synthase (iNOS) | M1 | $^{18}$F-NOS | Chemical | PET/CT | Lung inflammation | [123] |
| Cathepsin | M1/M2 | $^{68}$Ga-BMV101 | Chemical | PET/CT | Pulmonary fibrosis | [127] |

M1 macrophages [124–126]. Withana and colleagues generated a $^{64}$Cu labelled probe (BMV101) for targeting cysteine cathepsins for fibrosis PET imaging in pulmonary fibrosis patients demonstrating a three-fold greater radiotracer uptake in the patients' lungs compared to healthy controls [127].

*4.2.2. Macrophage targeted radiotracers in preclinical studies*

As described above, numerous macrophage targeted tracers are already clinically available, but the specificity of the tracers can still be improved for better diagnostic accuracy. Better and more specific radiotracers targeting for example SSTR, MMR and folate receptors are being developed and extensive research is currently focused on developing new macrophage targeted tracers targeting various other receptors and biological pathways (Table 4). A particularly interesting newly developed $^{18}$F-PEG-folate targeting FR-β has been reported to be more sensitive compared to $^{18}$F-FDG. It has also been shown to have a lower blood-pool radioactivity and 1.5 times improved target to background ratio compared to $^{11}$C-(R)-PK11195 [141,142]. Since $^{11}$C-(R)-PK11195 was already proven to be superior to $^{18}$F-FDG in LVV imaging, the new $^{18}$F-PEG-folate might prove to be useful in LVV imaging. Additionally, a shift towards peptide and antibody based radiotracers can be observed in current radiotracer developments with multiple studies showing promising results. Short peptides such as cinnamoyl-F-(D)L-F-(D)L-F (cFLFLF) and D-Ala1-peptide T-amide (DAPTA), formyl peptide receptor 1 (Fpr1) and chemokine receptor CCR5 antagonists were recently labelled with radioligands for macrophage imaging in murine models [145,146,149]. Radiotracers based on antibodies that bind to macrophage surface receptors such as CD163, CD11b, CD169 and CRIg have also been developed and studied in murine models of atherosclerosis, host versus graft disease and rheumatoid arthritis [145,147,148,151,152]. These peptide and antibody based radiotracers might exhibit higher specificity for macrophages compared to chemical radiotracers utilizing metabolic activity such as $^{18}$F-FDG, however they are large in size and therefore have poor tissue penetration ability and slow blood clearance.

Macrophages are phagocytic cells. Based on this principle, radiolabelled nanoparticles have been developed to target macrophages based on their ability to phagocytose these nanoparticles. Recently, Park et al. developed $^{89}$Zr-oxalate for PET imaging of rheumatoid arthritis in mouse models [156]. Small animal PET showed higher $^{89}$Zr-oxalate uptake compared to $^{18}$F-FDG in RA induced joints. Nahrendorf et al. developed a $^{64}$Cu labelled dextran-coated magnetic nanoparticle, $^{64}$Cu-TNP, which can be used for PET imaging as well as a contrast-enhancing agent for MRI [154]. In an atherosclerotic mouse model, $^{64}$Cu-TNP showed higher signals in atherosclerotic plaques when compared with $^{18}$F-FDG whereas histological examination revealed a direct correlation between $^{64}$Cu-TNP uptake and CD68$^{+}$ macrophages. This study illustrates the potential of macrophage specific radiotracers for the application of hybrid PET/MR imaging.

## 5. Future directions and theranostic applications

Good radiotracers should have a high affinity to its target, be highly specific, have rapid plasma clearance, possess a low radiation dose, and exhibit low toxicity [157–159]. Hence, designing a radiotracer requires thorough consideration of selecting target biomarkers or biological pathways, the ligand or molecule for radiolabelling, the target tissue, and also in determining suitable radionuclides. However, not all molecules are suitable for tagging with any readily available radionuclide. For example, tagging an antibody with the short half-life $^{11}$C

**Table 4**
Macrophage targeted radiotracers in preclinical studies.

| Tracer target | Dominant macrophage subset | Radiotracer | Type | Modality | Disease | Reference |
|---|---|---|---|---|---|---|
| Macrophage mannose receptor (MMR/CD206) | M2 | $^{64}$Cu-MAN-LIPs | Coated liposome | PET/MR | Tumour (TAMS imaging) | [128] |
| | | $^{99m}$Tc-anti MMR | Nanobody | SPECT/CT | Rheumatoid arthritis | [129] |
| | | $^{18}$F-FB-anti-MMR | Antibody fragment | PET | Tumour (TAMS imaging) | [130] |
| | | $^{68}$Ga-NOTA-MSA | Chemical | PET/CT | Atherosclerosis | [131] |
| | | $^{18}$F-FDM | Chemical | PET | Atherosclerosis | [132] |
| | | $^{18}$F-FDM | Chemical | PET/CT | Atherosclerosis | [133] |
| | | $^{111}$In-Tilmanocept | Chemical | SPECT | Atherosclerosis | [134] |
| Somatostatin receptor (SSTR) | M1 | $^{18}$F-FDR-NOC | Chemical | PET/CT | Atherosclerosis | [135] |
| Folate receptor beta (FR-β) | M2 | $^{99m}$Tc-his-folate | Chemical | SPECT/CT | Tumour (TAMS imaging) | [136] |
| | | $^{67}$Ga-DOTA-Bz-folate | Chemical | SPECT/CT | Tumour (TAMS imaging) | [137] |
| | | $^{111}$In-DTPA-folate | Chemical | SPECT/CT | Rheumatoid arthritis | [138] |
| | | $^{99m}$Tc-folate | Chemical | SPECT | Atherosclerosis | [139] |
| | | 3′-aza-2′-$^{18}$F-fluorofolicacid | Chemical | PET/CT | Tumour (TAMS imaging) | [140] |
| | | $^{18}$F-fluoro-PEG-folate | Chemical | PET | Rheumatoid arthritis | [141] |
| | | $^{18}$F-fluoro-PEG-folate | Chemical | PET/CT | Rheumatoid arthritis | [142] |
| CD80 | M1 | $^{11}$C-AM7 | Chemical | PET/CT | Atherosclerosis | [133] |
| | | $^{11}$C-AM7 | Chemical | PET/CT | Atherosclerosis | [143] |
| CD163 | M2 | $^{68}$Ga-ED2 | Antibody | PET | Rheumatoid arthritis | [144] |
| Formyl peptide receptor 1 (Fpr1) | M2 | cFLFLF-PEG-DOTA-$^{64}$Cu | Peptide | PET | Macrophage infiltration in diabetes | [145] |
| | | cFLFLF-PEG -$^{64}$Cu | Peptide | PET/CT | Osteoarthritis | [146] |
| CD11b | M1 | $^{99m}$Tc-MAG3-anti-CD11b | Antibody | SPECT/CT | Atherosclerosis | [147] |
| Siloadhesin (CD169) | M1 | $^{99m}$Tc-SER-4 | Antibody | SPECT/CT | Allograft rejection | [148] |
| CCR5 | M1 | $^{64}$Cu-DOTA-DAPTA | Peptide | PET/CT | Vascular injury | [149] |
| | | $^{64}$Cu-DOTA-DAPTA-comb | Peptide conjugated nanoparticles | PET/CT | Vascular injury | [149] |
| P32 protein | M1/M2 | $^{64}$Cu-LyP-1-dendrimer | Peptide labelled dendrimer | PET/CT | Atherosclerosis | [150] |
| CRIg (VSIG4) | M1/M2 | $^{99m}$Tc-anti-Vsig4-nanobody | Nanobody | SPECT/CT | Rheumatoid arthritis | [151] |
| | | $^{99m}$Tc-anti-Vsig4-nanobody | Nanobody | SPECT/CT | Hepatitis | [152] |
| P2X7 receptor | M1/M2 | $^{11}$C-GSK1482160 | Chemical | PET/CT | Neuro-inflammation | [153] |
| Macrophage phagocytosis | M1/M2 | $^{64}$Cu-TNP | Nanoparticle | PET/CT | Atherosclerosis | [154] |
| | | $^{89}$Zr-PL-HDL | Nanoparticle | PET | Tumour (TAMS imaging) | [155] |
| | | $^{89}$Zr-AI-HDL | Nanoparticle | PET | Tumour (TAMS imaging) | [155] |
| | | $^{89}$Zr-oxalate | Nanoparticle | PET | Tumour (TAMS imaging), tissue inflammation and rheumatoid arthritis | [156] |

radionuclide would yield an incompetent radiotracer since a viable antibody requires a longer period of distribution and tissue penetration time. The choice of radionuclide is also important in consideration of the target tissue. In general, sufficient time for blood clearance is preferred to lower the background blood-pool radioactivity. Depending on the molecule's blood clearance rate, some molecules with slower clearance rate are more suitable to be tagged with longer half-life radionuclides such as $^{18}$F while molecules with rapid blood clearance can be tagged with short half-life radionuclides such as $^{11}$C. In LVV imaging especially, rapid blood-pool clearance is a particularly important aspect to be taken into consideration in designing new radiotracers.

All radiotracers listed in Tables 2–4 are potentially applicable in LVV imaging. Theoretically, radiotracers targeting specific markers are better choices than radiotracers targeting metabolic activity. An example is the high background $^{18}$F-FDG uptake in other proliferating cells. Targeting TSPO has been proven to work in LVV imaging. Therefore, newly developed $^{18}$F-PBR06, $^{18}$F-FEDAC, $^{18}$F-FEDAA1106 and $^{18}$F-GE-180 may have a great potential for LVV imaging. Other clinically established radiotracers targeting SSTR such as $^{64}$Cu-DOTATATE and newly developed $^{18}$F-FDR-NOC may also prove to be useful in LVV imaging. $^{18}$F-PEG-folate which has been shown to be superior compared to first generation TSPO imaging tracers because of better target-to-background signal and might also be an interesting option for LVV imaging. However, although these tracer targets are highly expressed on activated macrophages, they are also expressed on other cells. Newer radiotracers such as $^{18}$F-NOS and $^{68}$Ga-pentixafor are more specific and may prove to be better macrophage targeted radiotracers although their suitability in imaging LVV has yet to be investigated. Antibody based radiotracers such as $^{68}$Ga-ED2 (anti CD163), $^{99m}$Tc-MAG3-anti-CD11b and $^{99m}$Tc-anti-Vsig4-nanobody could be superior to chemical based radiotracers because of their high specificity for macrophages. However, these radiotracers are large (150 kD) and will have problems penetrating the tissue and have yet to undergo clinical trials. Additionally, there is currently no available data showing the capability of these radiotracers in discriminating atherosclerosis and vasculitis. Since both of these diseases are characterized by the influx of macrophages and T-cells, it is important for future studies to distinguish the macrophage subsets and the difference in biomarker expression between the macrophages in atherosclerotic lesions and vasculitic lesions. It is also important to compare these radiotracers in both diseases to discover radiotracers capable of distinguishing vasculitic lesions and atherosclerotic lesions.

Radiolabelled antibodies may also shed new light in theranostic applications. Theranostics is a newly coined term that refers to a molecule that can act as both a diagnostic and therapeutic tool. Various theranostic radiopharmaceuticals have been developed for cancer therapy (for a comprehensive review see [160]). A possible theranostic approach in LVV may be to radiolabel specific therapeutic antibodies or drugs with radionuclides – thereby providing imaging capability and hence identification of the potential therapeutic target, followed by higher targeted, unlabelled therapeutic dose. This may support development of precision medicine. With regard to macrophages, macrophage targeted therapy has been proven to be effective in several inflammatory disorders with several newly developed macrophage targeted therapeutic antibodies and immunotoxins [161,162]. Radiolabelling these therapeutic agents may be an interesting prospective development in the theranostic field. However, it is currently unknown whether or not macrophage targeted therapy is beneficial in LVV. Further studies involving this modality in vasculitis should be carried out before theranostic applications can be considered.

## 6. Concluding remarks

Macrophages are important effector cells in the pathogenesis of large- and medium-vessel vasculitis and hence imaging macrophages is considered an effective tool in the diagnosis and monitoring of these diseases. Over the past decade, $^{18}$F-FDG PET has been proven to be a valuable modality in the early diagnosis of large vessel vasculitis but quickly loses its diagnostic accuracy following glucocorticoid treatment and less useful in monitoring long-term treatment follow-up of patients. As the main principle behind $^{18}$F-FDG PET is to image activated macrophages and lymphocytes, numerous well-established and newly emerging macrophage targeted radiotracers may prove to generate more favorable results than $^{18}$F-FDG PET in imaging LVV. Newer radiotracers such as $^{18}$F-PBR06, $^{64}$Cu-DOTATATE, $^{18}$F-PEG-FOLATE, $^{18}$F-NOS and $^{68}$Ga-pentixafor are more macrophage specific than $^{18}$F-FDG. Moreover, antibody based radiotracers such as $^{68}$Ga-ED2 (anti CD163) and $^{99m}$Tc-MAG3-anti-CD11b could even be better compared to chemical based radiotracers because of their high specificity. A drawback however, is that antibodies are large molecules which impairs tissue penetration. With regard to macrophage-targeted tracers, knowledge on macrophage subset distribution and their marker expression in LVV is currently limited. Therefore, future studies identifying macrophage phenotypes is required in order to cast a better understanding on the underlying pathogenesis of LVV and subsequently provide the necessary insight for better selection of tracers as well as new targets for tracer development.

### Take-home messages

- Macrophages as key players in the pathogenesis of LVV can be utilized as a diagnostic imaging target.
- $^{18}$F-FDG PET has proven to be useful in diagnostic imaging of LVV. However, this radiotracer is not specific and its diagnostic accuracy drops dramatically in patients undergoing glucocorticoid treatment.
- Macrophage targeted imaging utilizing radiotracers that target the TSPO receptor has proven to be valuable for LVV imaging.
- Macrophage targeted radiotracers developed for imaging cancer and inflammatory diseases can potentially be used for imaging LVV.

### Conflict of interest

The authors declare no conflict of interest.

### References

[1] Aird WC. Spatial and temporal dynamics of the endothelium. J Thromb Haemost 2005;3:1392–406.
[2] Weyand CM, Goronzy JJ. Immune mechanism in medium and large-vessel vasculitis. Nat Rev Rheumatol 2013;9:731–40.
[3] Jennette JC, Falk RJ, Bacon PA, Basu N, Cid MC, Ferrario F, et al. Revised International Chapel Hill consensus conference nomenclature of vasculitides. Arthritis Rheum 2012;65:1–11 (2013).
[4] Blockmans D, Knockaert D, Maes A, De Caestecker J, Stroobants S, Bobbaers H, et al. Clinical value of (18F) fluoro-deoxyglucose positron emission tomography for patients with fever of unknown origin. Clin Infect Dis 2001;32:191–6.
[5] Camici PG, Rimoldi OE, Gaemperli O, Libby P. Non-invasive anatomic and functional imaging of vascular inflammation and unstable plaque. Eur Heart J 2012;33:1309–17.
[6] Shimizu M, Inoue N, Mizuta M, Ikawa Y, Yachie A. Leopard skin appearance of cutaneous polyarteritis nodosa on 18Ffluorodeoxyglucose positron emission tomography. Rheumatology (Oxford) 2016;55:1090.
[7] Soussan M, Abisror N, Abad S, Nunes H, Terrier B, Pop G, et al. FDG-PET/CT in patients with ANCA associated vasculitis: case-series and literature review. Autoimmun Rev 2014;13:125–31.
[8] Kemna MJ, Vandergheynst F, Vöö S, Blocket D, Nguyen T, Timmermans S, et al. Positron emission tomography scanning in anti-neutrophil cytoplasmic antibodies-associated vasculitis. Medicine (Baltimore) 2015;94:e747.
[9] Ito K, Minamimoto R, Yamashita H, Yoshida S, Morooka M, Okasaki M, et al. Evaluation of Wegener's granulomatosis using 18F-fluorodeoxyglucose positron emission tomography/computed tomography. Ann Nucl Med 2013;27:209–16.
[10] Shirai T, Hilhorst M, Harrison DG, Goronzy JJ, Weyand CM. Macrophages in vascular inflammation – from atherosclerosis to vasculitis. Autoimmunity 2015;48(3):139–51.
[11] Salvarani C, Cantini F, Hunder GG. Polymyalgia rheumatica and giant-cell arteritis. Lancet 2008;372:234–45.
[12] Hunder GG, Bloch DA, Michel BA, Stevens MB, Arend WP, Calabrese LH, et al. The American College of Rheumatology 1990 criteria for the classification of giant cell arteritis. Arthritis Rheum 1990;33:1122–8.

[13] Arend WP, Michel BA, Bloch DA, Hunder GG, Calabrese LH, Edworthy SM, et al. The American College of Rheumatology 1990 criteria for the classification of Takayasu arteritis. Arthritis Rheum 1990;33:1129–34.
[14] Seyahi E. Takayasu arteritis: an update. Curr Opin Rheumatol 2017;29:51–6.
[15] Maffei Di Renzo M, Bova G, Auteri A, Pasqui AL. Takayasu's arteritis: a review of literature. Intern Emerg Med 2006;1(2):105–12.
[16] Chew SSL, Kerr NM, Danesh-Meyer HV. Giant cell arteritis. J Clin Nurosci 2009;16:1263–8.
[17] Dejaco C, Duftner C, Buttgereit F, Matteson EL, Dasgupta B. The spectrum of giant cell arteritis and polymyalgia rheumatica: revisiting the concept of the disease. Rheumatology 2017;56(4):506–15.
[18] Samson M, Audia S, Martin L, Janikashvili N, Bonnotte B. Pathogenesis of giant cell arteritis: new insight into the implication of CD161+ T cells. Clin Exp Rheumatol 2013;31(75):S65–73.
[19] Samson M, Corbera-Bellalta M, Audia S, Planas-Rigol E, Martin L, Cid MC, et al. Recent advances in our understanding of giant cell arteritis pathogenesis. Autoimmun Rev 2017;16:833–44.
[20] Ciccia F, Rizzo A, Ferrante A, Guggino G, Croci S, Cavazza A, et al. New insights into the pathogenesis of giant cell arteritis. Autoimmun Rev 2017;16:675–83.
[21] Wen Z, Shen Y, Berry G, Shahram F, Li Y, Watanabe R, et al. The microvasculature niche instructs T cells in large vessel vasculitis via the VEGF-Jagged1-Notch pathway. Sci Transl Med 2017;9:eaal3322.
[22] Watanabe R, Goronzy JJ, Berry G, Liao YJ, Weyand CM. Giant cell arteritis: from pathogenesis to therapeutic management. Curr Treatm Opt Rheumatol 2016;2(2):126–37.
[23] Van Sleen Y, Wang Q, van der Geest KSM, Westra J, Abdulahad WH, Heeringa P, et al. Involvement of monocyte subsets in the immunopathology of giant cell arteritis. Sci Rep 2017;7:6553.
[24] Shirai T, Hilhorst M, Harrison DG, Goronzy JJ, Weyand CM. Macrophages in vascular inflammation – from atherosclerosis to vasculitis. Autoimmunity 2015;48(3):139–51.
[25] Cochain C, Zernecke A. Macrophages in vascular inflammation and atherosclerosis. Eur J Physiol 2017;469:485–99.
[26] Weagel E, Smith C, Liu PG, Robison R, O'Neill K. Macrophage polarization and its role in cancer. J Clin Cell Immunol 2015;6:338.
[27] Laria A, Lurati A, Marrazza M, Mazzocchi D, Re KA, Scarpellini M. The macrophages in rheumatic diseases. J Inflamm Res 2016;9:1–11.
[28] Tabas I, Bornfeldt KE. Macrophage phenotype and function in different stages of atherosclerosis. Circ Res 2016;118(4):653–67.
[29] Erbel C, Akhavanpoor M, Okuyucu D, Wangler S, Dietz A, Zhao L, et al. IL-17A influences essential functions of the monocyte/macrophage lineage and is involved in advanced murine and human atherosclerosis. J Immunol 2014;193(9):4344–55.
[30] Martinez FO, Gordon S. The M1 and M2 paradigm of macrophage activation: time for reassessment. F1000Prime Rep, 6. ; 2014. p. 13.
[31] Vogel DY, Vereyken EJ, Glim JE, Heijnen PD, Moeton M, van der Valk P, et al. Macrophages in inflammatory multiple sclerosis lesions have an intermediate activation status. J Neuroinflammation 2013;10:35.
[32] Ciccia F, Alessandro R, Rizzo A, Raimondo S, Giardina A, Raiata F, et al. IL-33 is overexpressed in the inflamed arteries of patients with giant cell arteritis. Ann Rheum Dis 2013;72:258–64.
[33] Weyand CM, Goronzy JJ. Giant-cell arteritis and polymyalgia rheumatica. N Engl J Med 2014;371(1):50–7.
[34] Ninan j Lester S, Hill C. Giant cell arteritis. Best Pract Res Clin Rheumatol 2016;30(1):169–88.
[35] de Souza AWS, de Carvalho JF. Diagnostic and classification criteria of Takayasu arteritis. J Autoimmun 2014;48:79–83.
[36] Venketasubramanian N. Diagnosis and management of Takayasu arteritis. Pers Med 2012;1(1):255–6.
[37] Belhocine T, Blockmans D, Hustinx R, Vandevivere J, Mortelmans L. Imaging of large vessel vasculitis with $^{18}$FDG PET: illusion or reality? A critical review of the literature data. Eur J Nucl Med Mol Imaging 2003;30(9):1305–13.
[38] Holm PW, Sandovici M, Slart RHJA, Glaudemans AWJM, Rutgers A, Brouwer E. Vessel involvement in giant cell arteritis: an imaging approach. J Cardiovasc Surg (Torino) 2016;57(2):127–36.
[39] Luqmani R, Lee E, Singh S, Gillett M, Schmidt WA, Bradburn M, et al. The role of ultrasound compared to biopsy of temporal arteries in the diagnosis and treatment of giant cell arteritis (TABUL): a diagnostic accuracy and cost-effectiveness study. Health Technol Assess 2016;20(90):1–238.
[40] Masteling MG, Zeebregts CJ, Tio RA, Breek JC, Tietge UJF, de Boer JF, et al. High-resolution imaging of human atherosclerotic carotid plaques with micro18F-FDG PET scanning exploring plaque vulnerability. J Nucl Cardiol 2011;18(6):1066–75.
[41] Menezes LJ, Kotze CW, Agu O, Richards T, Brookes J, Goh VJ, et al. Investigating vulnerable atheroma using combined 18F-FDG PET/CT angiography of carotid plaque with immunohistochemical validation. J Nucl Med 2011;52(11):1698–703.
[42] Hag AM, Pedersen SF, Christoffersen C, Binderup T, Jensen MM, Jørgensen JT, et al. (18)F-FDG PET imaging of murine atherosclerosis: association with gene expression of key molecular markers. PLoS One 2012;7(11):e50908.
[43] Dunphy MP, Freiman A, Larson SM, Strauss HW. Association of vascular 18F-FDG uptake with vascular calcification. J Nucl Med 2005;46(8):1278–84.
[44] Bural GG, Torigian DA, Botvinick E, Houseni M, Basu S, Chen W, et al. A pilot study of changes in (18)F-FDG uptake, calcification and global metabolic activity of the aorta with aging. Hell J Nucl Med 2009;12(2):123–8.
[45] Pimlott S, Sutherland A. Molecular tracers for the PET and SPECT imaging of disease. Chem Soc Rev 2011;40:149–62.
[46] Garcia EV. Physical attributes, limitations, and future potential for PET and SPECT. J Nucl Cardiol 2012;19:S19–29.
[47] Prieto-González S, Espígol-Frigolé G, García-Martínez A, Alba MA, Tavera-Bahillo I, Hernández-Rodríguez J, et al. The expanding role of imaging in systemic vasculitis. Rheum Dis Clin North Am 2016;42(4):733–51.
[48] Camici PG, Rimoldi OE, Gaemperli O, Libby P. Non-invasive anatomic and functional imaging of vascular inflammation and unstable plaque. Eur Heart J 2012;33:1309–17.
[49] Lee TC, Alessio AM, Miyaoka RM, Kinahan PE. Morphology supporting function: attenuation correction for SPECT/CT, PET/CT, and PET/MR imaging. Q J Nucl Med Mol Imaging 2016;60(1):25–39.
[50] Gaemperli O, Boyle JJ, Rimoldi OE, Mason JC, Camici PG. Molecular imaging of vascular inflammation. Eur J Nucl Med Mol Imaging 2010;36(6):1236-36.
[51] Rahmim A, Zaidi H. PET versus SPECT: strengths, limitations and challenges. Nucl Med Commun 2008;29:193–207.
[52] Takahashi A, Himuro K, Yamashita Y, Komiya I, Baba S, Sasaki M. Monte Carlo simulation of PET and SPECT imaging of 90Y. Med Phys 2015;42(4):1926–35.
[53] Meikle SR, Kench P, Kassiou M, Banati RB. Small animal SPECT and its place in the matrix of molecular imaging technologies. Phys Med Biol 2005;50:R45-1.
[54] Caobelli F, Bengel FM. In vivo evaluation of atherosclerotic plaques and culprit lesions using noninvasive techniques. Nat Rev Cardiol 2015;12:79.
[55] Blockmans D, Maes A, Stroobants S, Nuyts J, Bormans G, Knockaert D, et al. New arguments for a vasculitic nature of polymyalgia rheumatica using positron emission tomography. Rheumatology (Oxford) 1999;38:444–7.
[56] Meller J, Strutz F, Siefker U, Scheel A, Sahlmann CO, Lehmann K, et al. Early diagnosis and follow-up of aortitis with [(18)F]FDG PET and MRI. Eur J Nucl Med Mol Imaging 2003;30:730–6.
[57] Hautzel H, Sander O, Heinzel A, Schneider M, Müller HW. Assessment of large-vessel involvement in giant cell arteritis with 18F-FDG PET: introducing an ROC-analysis-based cutoff ratio. J Nucl Med 2008;49:1107–13.
[58] Besson FL, de Boysson H, Parienti JJ, Bouvard G, Bienvenu B, Agostini D. Towards an optimal semiquantitative approach in giant cell arteritis: an (18)F-FDG PET/CT case-control study. Eur J Nucl Med Mol Imaging 2014;41:155–66.
[59] Stellingwerf MD, Brouwer E, Lensen KDF, Rutgers A, Arends S, van der Geest KSM, et al. Different scoring methods of FDG PET/CT in giant cell arteritis need for standardization. Medicine 2015;94:37.
[60] Clifford AH, Murphy EM, Burrell SC, Bligh MP, MacDougall RF, Heathcote JG, et al. Positron emission tomography/computerized tomography in newly diagnosed patients with giant cell arteritis who are taking glucocorticoids. J Rheumatol 2017;44(12).
[61] Blockmans D, de Ceuninck L, Vanderschueren S, Knockaert D, Mortelmans L, Bobbaers H. Repetitive 18F-fluorodeoxyglucose positron emission tomography in giant cell arteritis: a prospective study of 35 patients. Arthritis Rheum 2006;55:131–7.
[62] Maleszewski JJ, Younge BR, Fritzlen JT, Hunder GG, Goronzy JJ, Warrington KJ, et al. Clinical and pathological evolution of giant cell arteritis: a prospective study of follow-up temporal artery biopsies in 40 treated patients. Mod Pathol 2017;30(6):788–96.
[63] Canat X, Guillaumont A, Bouaboula M, Poinot-Chazel C, Derocq JM, Carayon P, et al. Peripheral benzodiazepine receptor modulation with phagocyte differentiation. Biochem Pharmacol 1993;46(3):551–4.
[64] Kim EJ, Yu SW. Translocator protein 18 kDa (TSPO): old dogma, new mice, new structure, and new questions for neuroprotection. Neural Regen Res 2015;10(6):878–80.
[65] Vas Á, Shchukin Y, Karrenbauer VD, Cselényi Z, Kostulas K, Hillert J, et al. Functional neuroimaging in multiple sclerosis with radiolabelled glia markers: preliminary comparative PET studies with [11C]vinpocetine and [11C]PK11195 in patients. J Neurol Sci 2008;264(1–2):9–17.
[66] Chauveau F, Van Camp N, Dollé F, Kuhnast B, Hinnen F, Damont A, et al. Comparative evaluation of the translocator protein radioligands 11C-DPA-713, 18F-DPA-714, and 11C-PK11195 in a rat model of acute neuroinflammation. J Nucl Med 2009;50(3):468–76.
[67] Pugliese F, Gaemperli O, Kinderlerer AR, Lamare F, Shalhoub J, et al. Imaging of vascular inflammation with [11C]-PK11195 and positron emission tomography/computed tomography angiography. J Am Coll Cardiol 2010;56(8):653–61.
[68] Chauveau F, Boutin H, Van Camp N, Thominiaux C, Hantraye P, Rivron L, et al. In vivo imaging of neuroinflammation in the rodent brain with [11C]SSR180575, a novel indoleacetamide radioligand of the translocator protein (18 kDa). Eur J Nucl Med Mol Imaging 2011;38:509–14.
[69] Gaemperli O, Shalhoub J, Owen DR, Lamare F, Johansson S, Fouladi N, et al. Imaging intraplaque inflammation in carotid atherosclerosis with 11C-PK11195 positron emission tomography/computed tomography. Eur Heart J 2012;33(15):1902–10.
[70] Boutin H, Prenant C, Maroy R, Galea J, Greenhalgh AD, Smigova A, et al. [18F]DPA-714: direct comparison with [11C]PK11195 in a model of cerebral ischemia in rats. PLoS One 2013;8(2):e56441.
[71] van der Laken CJ, Elzinga EH, Kropholler MA, Molthoff CF, van der Heijden JW, Maruyama K, et al. Noninvasive imaging of macrophages in rheumatoid synovitis using 11C-(R)-PK11195 and positron emission tomography. Arthritis Rheum 2008;58(11):3350–5.
[72] Lamare F, Hinz R, Gaemperli O, Pugliese F, Mason JC, Spinks T, et al. Detection and quantification of large-vessel Inflammation with 11C-(R)-PK11195 PET/CT. J Nucl Med 2010;52(1):33–9.
[73] Folkersma H, Foster Dingley JC, van Berckel BN, Rozemuller A, Boellaard R, Huisman MC, et al. Increased cerebral (R)-[11C]PK11195 uptake and glutamate release in a rat model of traumatic brain injury: a longitudinal pilot study. J Neuroinflammation 2011;8:67.
[74] Ratchford JN, Endres CJ, Hammoud DA, Pomper MG, Shiee N, McGready J, et al. Decreased microglial activation in MS patients treated with glatiramer acetate. J Neurol 2012;259(6):1199–205.

[75] Hatori A, Yui J, Yamasaki T, Xie L, Kumata K, Fujinaga M, et al. PET imaging of lung inflammation with [18F]FEDAC, a radioligand for translocator protein (18 kDa). PLoS One 2012;7(9):e45065.
[76] Hatori A, Yui J, Xie L, Yamasaki T, Kumata K, Fujinaga M, et al. Visualization of acute liver damage induced by cycloheximide in rats using PET with [18F]FEDAC, a radiotracer for translocator protein (18 kDa). PLoS One 2014;9(1):e86625.
[77] Gent YYJ, ter Wee MM, Voskuyl AE, den Uyl D, Ahmadi N, Dowling C, et al. Subclinical synovitis detected by macrophage PET, but not MRI, is related to short-term flare of clinical disease activity in early RA patients: an exploratory study. Arthritis Res Ther 2015;17:266.
[78] Boutin H, Murray K, Pradillo J, Maroy R, Smigova A, Gerhard A, et al. 18F-GE-180: a novel TSPO radiotracer compared to 11C-R-PK11195 in a preclinical model of stroke. Eur J Nucl Med Mol Imaging 2015;42(3):503–11.
[79] Sarda-Mantel L, Alsac J, Boisgard R, Hervatin F, Montravers F, Tavitian B, et al. Comparison of 18F-fluoro-deoxy-glucose, 18F-fluoro-methyl-choline, and 18F-DPA714 for positron-emission tomography imaging of leukocyte accumulation in the aortic wall of experimental abdominal aneurysms. J Vasc Surg 2012;56(3):765–73.
[80] Abourbeh G, Thézé B, Maroy R, Dubois A, Brulon V, Fontyn Y, et al. Imaging microglial/macrophage activation in spinal cords of experimental autoimmune encephalomyelitis rats by positron emission tomography using the mitochondrial 18 kDa translocator protein radioligand [$^{18}$F]DPA-714. J Neurosci 2012;32(17):5728–36.
[81] Wu C, Yue X, Lang L, Kiesewetter DO, Li F, Zhu Z, et al. Longitudinal PET imaging of muscular inflammation using 18F-DPA-714 and 18F-Alfatide II and differentiation with tumors. Theranostics 2014;4(5):546–55.
[82] Pottier G, Bernards N, Dollé F, Boisgard R. [$^{18}$F]DPA-714 as a biomarker for positron emission tomography imaging of rheumatoid arthritis in an animal model. Arthritis Res Ther 2014;16(2):R69.
[83] Kashiyama N, Miyagawa S, Fukushima S, Kawamura T, Kawamura A, Yoshida S, et al. Development of PET imaging to visualize activated macrophages accumulated in the transplanted iPSc-derived cardiac myocytes of allogeneic origin for detecting the immune rejection of allogeneic cell transplants in mice. PLoS One 2016;11(12):e0165748.
[84] Israel I, Ohsiek A, Al-Momani E, Albert-Weissenberger C, Stetter C, Mencl S, et al. Combined [18F]DPA-714 micro-positron emission tomography and autoradiography imaging of microglia activation after closed head injury in mice. J Neuroinflammation 2016;13:140.
[85] Oh U, Fujita M, Ikonomidou VN, Evangelou IE, Matsuura E, Harberts E, et al. Translocator protein PET imaging for glial activation in multiple sclerosis. J Neuroimmune Pharmacol 2011;6(3):354–61.
[86] Shao X, Wang X, English SJ, Desmond T, Sherman PS, Quesada CA, et al. Imaging of carrageenan-induced local inflammation and adjuvant-induced systemic arthritis with [11C]PBR28 PET. Nucl Med Biol 2013;40(7):906–11.
[87] Dedeurwaerdere S, Callaghan PD, Pham T, Rahardjo GL, Amhaoul H, Berghofer P, et al. PET imaging of brain inflammation during early epileptogenesis in a rat model of temporal lobe epilepsy. EJNMMI Res 2012;2:60.
[88] Mattner F, Staykova M, Berghofer P, Wong HJ, Fordham S, Callaghan P, et al. Central nervous system expression and PET imaging of the translocator protein in relapsing-remitting experimental autoimmune encephalomyelitis. J Nucl Med 2013;54(2):291–8.
[89] Colasanti A, Guo Q, Muhlert N, Giannetti P, Onega M, Newbould RD, et al. In vivo assessment of brain white matter inflammation in multiple sclerosis with (18)F-PBR111 PET. J Nucl Med 2014;55(7):1112–8.
[90] Fujimura Y, Zoghbi SS, Simèon FG, Taku A, Pike VW, Innis RB, et al. Quantification of translocator protein (18 kDa) in the human brain with pet and a novel radioligand, 18F-PBR06. J Nucl Med 2009;50(7):1047–53.
[91] Takano A, Piehl F, Hillert J, Varrone A, Nag S, Gulyás B, et al. In vivo TSPO imaging in patients with multiple sclerosis: a brain PET study with [18F]FEDAA1106. EJNMMI Res 2013;3:30.
[92] Cuhlmann S, Gsell W, Van der Heiden K, Habib J, Tremoleda JL, Khalil M, et al. In vivo mapping of vascular inflammation using the translocator protein tracer 18F-FEDAA1106. Mol Imaging 2014;13:1–11.
[93] Xie L, Yamasaki T, Ichimaru N, Yui J, Kawamura K, Kumata K, et al. [(11)C]DAC-PET for noninvasively monitoring neuroinflammation and immunosuppressive therapy efficacy in rat experimental autoimmune encephalomyelitis model. J Neuroimmune Pharmacol 2013;7(1):231–42.
[94] Foss CA, Harper JS, Wang H, Pomper MG, Jain SK. Noninvasive molecular imaging of tuberculosis-associated inflammation with radioiodinated DPA-713. J Infect Dis 2013;208(12):2067–74.
[95] Foss CA, Bedja D, Mease RC, Wang H, Kass DA, Chatterjee S, et al. Molecular imaging of inflammation in the ApoE−/− mouse model of atherosclerosis with IodoDPA. Biochem Biophys Res Commun 2015;461(1):70–5.
[96] Foss CA, Liu L, Mease RC, Wang H, Pasricha P, Pomper MG. Imaging macrophage accumulation in a murine model of chronic pancreatitis with [125I]iodoDPA SPECT-CT. J Nucl Med 2017;8 (pii:jnumed.117.189571).
[97] Owen DRJ, Gunn RN, Rabiner EA, Bennacef I, Fujita M, Kreisl WC, et al. Mixed-affinity binding in humans with 18-kDa translocator protein ligands. J Nucl Med 2011;52(1):24–32.
[98] Owen DR, Yeo AJ, Gunn RN, Song K, Wadsworth G, Lewis A, et al. An 18-kDa translocator protein (TSPO) polymorphism explains differences in binding affinity of the PET radioligand PBR28. J Cereb Blood Flow Metab 2012;32(1):1–5.
[99] Li X, Samnick S, Lapa C, Israel I, Buck AK, Kreissl MC, et al. 68Ga-DOTATATE PET/CT for the detection of inflammation of large arteries: correlation with18F-FDG, calcium burden and risk factors. EJNMMI Res 2012;2:52.
[100] Malmberg C, Ripa RS, Johnbeck CB, Knigge U, Langer SW, Mortensen J, et al. 64Cu-DOTATATE for noninvasive assessment of atherosclerosis in large arteries and its correlation with risk factors: head-to-head comparison with 68Ga-DOTATOC in 60 patients. J Nucl Med 2015;56(12):1895–900.
[101] Pedersen SF, Sandholt BV, Keller SH, Hansen AE, Clemmensen AE, Sillesen H, et al. 64Cu-DOTATATE PET/MRI for detection of activated macrophages in carotid atherosclerotic plaques: studies in patients undergoing endarterectomy. Arterioscler Thromb Vasc Biol 2015;35(7):1696–703.
[102] Gormsen LC, Haraldsen A, Kramer S, Dias AH, Kim WY, Borghammer P. A dual tracer 68Ga-DOTANOC PET/CT and 18F-FDG PET/CT pilot study for detection of cardiac sarcoidosis. EJNMMI Res 2016;6:52.
[103] Tarkin JM, Joshi FR, Evans NR, Chowdhury MM, Figg NL, Shah AV, et al. Detection of atherosclerotic inflammation by 68Ga-DOTATATE PET compared to [18F]FDG PET imaging. J Am Coll Cardiol 2017;69(14):1774–91.
[104] Zanni MV, Toribio M, Wilks MQ, Lu MT, Burdo TH, Walker J, et al. Application of a novel CD206+ macrophage-specific arterial imaging strategy in HIV-infected individuals. J Infect Dis 2017;215(8):1264–9.
[105] Contento RL, Molon B, Boularan C, Pozzan T, Manes S, Marullo S, et al. CXCR4–CCR5: a couple modulating T cell functions. Proc Natl Acad Sci U S A 2008;105(29):10101–6.
[106] Wang XF, Wang HS, Wang H, Zhang F, Wang KF, Guo Q, et al. The role of indoleamine 2,3-dioxygenase (IDO) in immune tolerance: focus on macrophage polarization of THP-1 cells. Cell Immunol 2014;289(1-2):42–8.
[107] Hyafil F, Pelisek J, Laitinen I, Schottelius M, Mohring M, Döring Y, et al. Imaging the cytokine receptor CXCR4 in atherosclerotic plaques with the radiotracer 68Ga-pentixafor for PET. J Nucl Med 2017;58(3):499–506.
[108] Jager NA, Teteloshvili N, Zeebregts CJ, Westra J, Bijl M. Macrophage folate receptor-β (FR-β) expression in auto-immune inflammatory rheumatic diseases: a forthcoming marker for cardiovascular risk? Autoimmun Rev 2012;11(9):621–6.
[109] Van De Wiele C, Sathekge M, Maes A. Targeting monocytes and macrophages by means of SPECT and PET. Q J Nucl Med Mol Imaging 2014;58(3):269–75.
[110] Tsuneyoshi Y, Tanaka M, Nagai T, Sunahara N, Matsuda T, Sonoda T, et al. Functional folate receptor beta-expressing macrophages in osteoarthritis synovium and their M1/M2 expression profiles. Scand J Rheumatol 2012;41(2):132–40.
[111] Vöö S, Kwee RM, Sluimer JC, Schreuder FH, Wierts R, Bauwens M, et al. Imaging intraplaque inflammation in carotid atherosclerosis with 18F-fluorocholine positron emission tomography-computed tomography: prospective study on vulnerable atheroma with immunohistochemical validation. Circ Cardiovasc Imaging 2016;9(5) (pii:e004467).
[112] Matteson EL, Lowe VJ, Prendergast FG, Crowson CS, Moder KG, Morgenstern DE, et al. Assessment of disease activity in rheumatoid arthritis using a novel folate targeted radiopharmaceutical Folatescan™. Clin Exp Rheumatol 2009;27(2):253–9.
[113] Lo M, Wang YZ, Gout PW. The x(c)-cystine/glutamate antiporter: a potential target for therapy of cancer and other diseases. J Cell Physiol 2008;215(3):593–602.
[114] Sato H, Fujiwara K, Sagara J, Bannai S. Induction of cystine transport activity in mouse peritoneal macrophages by bacterial lipopolysaccharide. Biochem J 1995;310(Pt 2):547–51.
[115] Chae SY, Choi CM, Shim TS, Park Y, Park CS, Lee HS, et al. Exploratory clinical investigation of (4S)-4-(3-18F-fluoropropyl)-L-glutamate PET of inflammatory and infectious lesions. J Nucl Med 2016;57(1):67–9.
[116] Kubota R, Kubota K, Yamada S, Tada M, Takahashi T, Iwata R, et al. Methionine uptake by tumor tissue: a microautoradiographic comparison with FDG. J Nucl Med 1995;36(3):484–92.
[117] Morooka M, Kubota K, Kadowaki H, Ito K, Okazaki O, Kashida M, et al. 11C-methionine PET of acute myocardial infarction. J Nucl Med 2009;50(8):1283–7.
[118] Maya Y, Werner RA, Schütz C, Wakabayashi H, Samnick S, Lapa C, et al. 11C-methionine PET of myocardial inflammation in a rat model of experimental autoimmune myocarditis. J Nucl Med 2016;57(12):1985–90.
[119] Thackeray JT, Bankstahl JP, Wang Y, Wollert KC, Bengel FM. Targeting amino acid metabolism for molecular imaging of inflammation early after myocardial infarction. Theranostics 2016;6(11):1768–79.
[120] Kleinert H, Schwarz PM, Förstermann U. Regulation of the expression of inducible nitric oxide synthase. Biol Chem 2003;384(10-11):1343–64.
[121] Förstermann U, Sessa WC. Nitric oxide synthases: regulation and function. Eur Heart J 2012;33(7):829–37.
[122] Stöger JL, Gijbels MJ, van der Velden S, Manca M, van der Loos CM, Biessen EA, et al. Distribution of macrophage polarization markers in human atherosclerosis. Atherosclerosis 2012;225(2):461–8.
[123] Huang HJ, Isakow W, Byers DE, Engle JT, Griffin EA, Kemp D, et al. Imaging pulmonary inducible nitric oxide synthase expression with PET. J Nucl Med 2015;56(1):76–81.
[124] Gocheva V, Wang HW, Gadea BB, Shree T, Hunter KE, Garfall AL, et al. A. IL-4 induces cathepsin protease activity in tumor-associated macrophages to promote cancer growth and invasion. Genes Dev 2010;24(3):241–55.
[125] Conus S, Simon HU. Cathepsins and their involvement in immune responses. Swiss Med Wkly 2010;140:w13042.
[126] Genin M, Clement F, Fattaccioli A, Raes M, Michiels C. M1 and M2 macrophages derived from THP-1 cells differentially modulate the response of cancer cells to etoposide. BMC Cancer 2015;15:577.
[127] Withana NP, Ma X, McGuire HM, Verdoes M, van der Linden WA, Ofori LO, et al. Non-invasive imaging of idiopathic pulmonary fibrosis using cathepsin protease probes. Sci Rep 2016;6:19755.
[128] Locke LW, Mayo MW, Yoo AD, Williams MB, Berr SS. PET imaging of tumor associated macrophages using mannose coated 64Cu liposomes. Biomaterials 2012;33(31):7785–93.
[129] Put S, Schoonooghe S, Devoogdt N, Schurgers E, Avau A, Mitera T, et al. SPECT imaging of joint inflammation with nanobodies targeting the macrophage mannose

receptor in a mouse model for rheumatoid arthritis. J Nucl Med 2013;54(5):807–14.
[130] Blykers A, Schoonooghe S, Xavier C, D'hoe K, Laoui D, D'Huyvetter M, et al. PET imaging of macrophage mannose receptor-expressing macrophages in tumor stroma using 18F-radiolabeled camelid single-domain antibody fragments. J Nucl Med 2015;56(8):1265–71.
[131] Kim EJ, Kim S, Seo HS, Lee YJ, Eo JS, Jeong JM, et al. Novel PET imaging of atherosclerosis with 68Ga-labeled NOTA-neomannosylated human serum albumin. J Nucl Med 2016;57(11):1792–7.
[132] Tahara N, Mukherjee J, de Haas HJ, Petrov AD, Tawakol A, Haider N, et al. 2-deoxy-2-[18F]fluoro-D-mannose positron emission tomography imaging in atherosclerosis. Nat Med 2014;20(2):215–9.
[133] Meletta R, Steier L, Borel N, Mu L, Keller C, Chiotellis A, et al. CD80 is upregulated in a mouse model with shear stress-induced atherosclerosis and allows for evaluating CD80-targeting PET tracers. Mol Imaging Biol 2017;19(1):90–9.
[134] Varasteh Z, Hyafil F, Anizan N, Diallo D, Aid-Launais R, Mohanta S, et al. Targeting mannose receptor expression on macrophages in atherosclerotic plaques of apolipoprotein E-knockout mice using 111In-tilmanocept. EJNMMI Res 2017;7:40.
[135] Rinne P, Hellberg S, Kiugel M, Virta J, Li XG, Käkelä M, et al. Comparison of somatostatin receptor 2-targeting PET tracers in the detection of mouse atherosclerotic plaques. Mol Imaging Biol 2016;18(1):99–108.
[136] Müller C, Forrer F, Schibli R, Krenning EP, de Jong M. SPECT study of folate receptor-positive malignant and normal tissues in mice using a novel 99mTc-radiofolate. J Nucl Med 2008;49(2):310–7.
[137] Müller C, Vlahov IR, Santhapuram HK, Leamon CP, Schibli R. Tumor targeting using 67Ga-DOTA-Bz-folate–investigations of methods to improve the tissue distribution of radiofolates. Nucl Med Biol 2011;38(5):715–23.
[138] Piscaer TM, Müller C, Mindt TL, Lubberts E, Verhaar JA, Krenning EP, et al. Imaging of activated macrophages in experimental osteoarthritis using folate-targeted animal single-photon-emission computed tomography/computed tomography. Arthritis Rheum 2011;63(7):1898–907.
[139] Jager NA, Westra J, Golestani R, van Dam GM, Low PS, Tio RA, et al. Folate receptor-β imaging using 99mTc-folate to explore distribution of polarized macrophage populations in human atherosclerotic plaque. J Nucl Med 2014;55(12):1945–51.
[140] Betzel T, Müller C, Groehn V, Müller A, Reber J, Fischer CR, et al. Radiosynthesis and preclinical evaluation of 3′-Aza-2′-[18F]fluorofolic acid: a novel PET radiotracer for folate receptor targeting. Bioconjug Chem 2013;24:205–14.
[141] Gent YY, Weijers K, Molthoff CF, Windhorst AD, Huisman MC, Smith DE, et al. Evaluation of the novel folate receptor ligand [18F]fluoro-PEG-folate for macrophage targeting in a rat model of arthritis. Arthritis Res Ther 2013;15(2):R37.
[142] Chandrupatla DMSH, Jansen G, Vos R, Verlaan M, Chen Q, Low PS, et al. In-vivo monitoring of anti-folate therapy in arthritic rats using [18F]fluoro-PEG-folate and positron emission tomography. Arthritis Res Ther 2017;19(1):114.
[143] Müller A, Mu L, Meletta R, Beck K, Rancic Z, Drandarov K, et al. Towards non-invasive imaging of vulnerable atherosclerotic plaques by targeting co-stimulatory molecules. Int J Cardiol 2014;174(3):503–15.
[144] Eichendorff S, Svendsen P, Bender D, Keiding S, Christensen EI, Deleuran B, et al. Biodistribution and PET imaging of a novel [68Ga]-anti-CD163-antibody conjugate in rats with collagen-induced arthritis and in controls. Mol Imaging Biol 2015;17(1):87–93.
[145] Zhang Y, Kundu B, Zhong M, Huang T, Li J, Chen MH, et al. PET imaging detection of macrophages with a formyl peptide receptor antagonist. Nucl Med Biol 2015;42(4):381–6.
[146] Yang X, Chordia MD, Du X, Graves JL, Zhang Y, Park YS, et al. Targeting formyl peptide receptor 1 of activated macrophages to monitor inflammation of experimental osteoarthritis in rat. J Orthop Res 2016;34(9):1529–38.
[147] Liu G, Hu Y, Xiao J, Li X, Li Y, Tan H, et al. 99mTc-labelled anti-CD11b SPECT/CT imaging allows detection of plaque destabilization tightly linked to inflammation. Sci Rep 2016;6:20900.
[148] O'Neill ASG, Terry SYA, Brown K, Meader L, Wong AMS, Cooper JD, et al. Non-invasive molecular imaging of inflammatory macrophages in allograft rejection. EJNMMI Res 2015;5:69.
[149] Luehmann HP, Pressly ED, Detering L, Wang C, Pierce R, Woodard PK, et al. PET/CT imaging of chemokine receptor CCR5 in vascular injury model using targeted nanoparticle. J Nucl Med 2014;55(4):629–34.
[150] Seo JW, Baek H, Mahakian LM, Kusunose J, Hamzah J, Ruoslahti E, et al. W. $^{64}$Cu-Labeled LyP-1-dendrimer for PET-CT imaging of atherosclerotic plaque. Bioconjug Chem 2014;25(2):231–9.
[151] Zheng F, Put S, Bouwens L, Lahoutte T, Matthys P, Muyldermans S, et al. Molecular imaging with macrophage CRIg-targeting nanobodies for early and preclinical diagnosis in a mouse model of rheumatoid arthritis. J Nucl Med 2014;55(5):824–9.
[152] Zheng F, Devoogdt N, Sparkes A, Morias Y, Abels C, Stijlemans B, et al. Monitoring liver macrophages using nanobodies targeting Vsig4: concanavalin A induced acute hepatitis as paradigm. Immunobiology 2015;220(2):200–9.
[153] Territo PR, Meyer JA, Peters JS, Riley AA, McCarthy BP, Gao M, et al. Characterization of 11C-GSK1482160 for targeting the P2X7 receptor as a biomarker for neuroinflammation. J Nucl Med 2017;58(3):458–65.
[154] Nahrendorf M, Zhang H, Hembrador S, Panizzi P, Sosnovik DE, Aikawa E, et al. Nanoparticle PET-CT imaging of macrophages in inflammatory atherosclerosis. Circulation 2008;117(3):379–87.
[155] Pérez-Medina C, Tang J, Abdel-Atti D, Hogstad B, Merad M, Fisher EA, et al. PET imaging of tumor-associated macrophages with 89Zr-labeled high-density lipoprotein nanoparticles. J Nucl Med 2015;56(8):1272–7.
[156] Park JA, Lee YJ, Lee JW, Yoo RJ, Shin UC, Lee KC, et al. Evaluation of [(89)Zr]-oxalate as a PET tracer in inflammation, tumor, and rheumatoid arthritis models. Mol Pharm 2016;13(7):2571–7.
[157] Sharma R, Aboagye E. Development of radiotracers for oncology – the interface with pharmacology. Br J Pharmacol 2011;163(8):1565–85.
[158] Zanotti-Fregonara P, Innis RB. Suggested pathway to assess radiation safety of 11C-labeled PET tracers for first-in-human studies. Eur J Nucl Med Mol Imaging 2012;39(3):544–7.
[159] Zanotti-Fregonara P, Lammertsma AA, Innis RB. Suggested pathway to assess radiation safety of 18F-labeled PET tracers for first-in-human studies. Eur J Nucl Med Mol Imaging 2013;40(11). https://doi.org/10.1007/s00259-013-2512-x.
[160] Drude N, Tienken L, Mottaghy FM. Theranostic and nanotheranostic probes in nuclear medicine. Methods 2017;130:14–22.
[161] Ries CH, Cannarile MA, Hoves S, Benz J, Wartha K, Runza V, et al. Targeting tumor-associated macrophages with anti-CSF-1R antibody reveals a strategy for cancer therapy. Cancer Cell 2014;25(6):846–59.
[162] Akinrinmade OA, Chetty S, Daramola AK, Islam M, Thepen T, Barth S. CD64: an attractive immunotherapeutic target for M1-type macrophage mediated chronic inflammatory diseases. Biomedicine 2017;5(3):56.